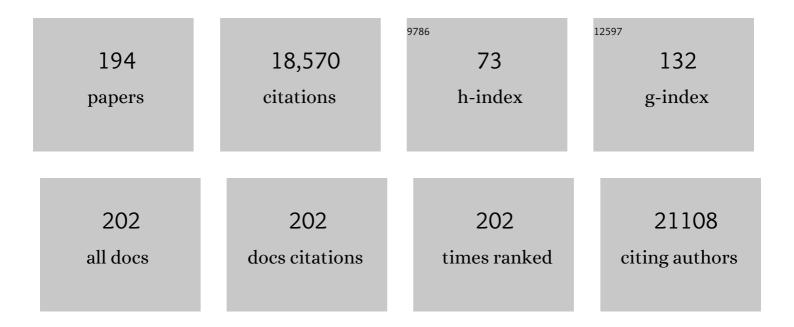
List of Publications by Year in descending order

Source: https://exaly.com/author-pdf/5917815/publications.pdf Version: 2024-02-01



#	Article	IF	CITATIONS
1	Ultrasmall superparamagnetic iron oxide nanoparticles: A next generation contrast agent for magnetic resonance imaging. Wiley Interdisciplinary Reviews: Nanomedicine and Nanobiotechnology, 2022, 14, e1740.	6.1	60
2	Anchoring Group-Mediated Radiolabeling of Inorganic Nanoparticles─A Universal Method for Constructing Nuclear Medicine Imaging Nanoprobes. ACS Applied Materials & Interfaces, 2022, 14, 8838-8846.	8.0	19
3	Twoâ€Pronged Intracellular Coâ€Delivery of Antigen and Adjuvant for Synergistic Cancer Immunotherapy. Advanced Materials, 2022, 34, e2202168.	21.0	41
4	Near-Infrared Afterglow Luminescence of Chlorin Nanoparticles for Ultrasensitive <i>In Vivo</i> Imaging. Journal of the American Chemical Society, 2022, 144, 6719-6726.	13.7	51
5	Healing Diabetic Ulcers with MoO _{3â^'} <i>_X</i> Nanodots Possessing Intrinsic ROSâ€5cavenging and Bacteriaâ€Killing Capacities. Small, 2022, 18, e2107137.	10.0	30
6	Bright, Magnetic NIR-II Quantum Dot Probe for Sensitive Dual-Modality Imaging and Intensive Combination Therapy of Cancer. ACS Nano, 2022, 16, 8076-8094.	14.6	31
7	An APNâ€Activated Chemiluminescent Probe for Imageâ€Guided Surgery of Malignant Tumors. Advanced Optical Materials, 2022, 10, .	7.3	14
8	Quantitative Mapping of Glutathione within Intracranial Tumors through Interlocked MRI Signals of a Responsive Nanoprobe. Angewandte Chemie - International Edition, 2021, 60, 8130-8138.	13.8	57
9	Recent Advances in Renal Clearable Inorganic Nanoparticles for Cancer Diagnosis. Particle and Particle Systems Characterization, 2021, 38, 2000270.	2.3	8
10	Quantitative Mapping of Glutathione within Intracranial Tumors through Interlocked MRI Signals of a Responsive Nanoprobe. Angewandte Chemie, 2021, 133, 8211-8219.	2.0	6
11	Two-Dimensional and Subnanometer-Thin Quasi-Copper-Sulfide Semiconductor Formed upon Copper–Copper Bonding. ACS Nano, 2021, 15, 873-883.	14.6	12
12	Quantitatively visualizing the activity of MMP-2 enzyme in vivo using a ratiometric photoacoustic probe. Methods in Enzymology, 2021, 657, 59-87.	1.0	2
13	Turning-on persistent luminescence out of chromium-doped zinc aluminate nanoparticles by instilling antisite defects under mild conditions. Nanoscale, 2021, 13, 8514-8523.	5.6	10
14	A Cyclodextrinâ€Hosted Ir(III) Complex for Ratiometric Mapping of Tumor Hypoxia In Vivo. Advanced Science, 2021, 8, 2004044.	11.2	22
15	X-ray-Based Techniques to Study the Nano–Bio Interface. ACS Nano, 2021, 15, 3754-3807.	14.6	60
16	A Pretargeting Strategy Enabled by Bioorthogonal Reactions Towards Advanced Nuclear Medicines: Application and Perspective. Chemical Research in Chinese Universities, 2021, 37, 870-879.	2.6	2
17	Furin Enzyme and pH Synergistically Triggered Aggregation of Gold Nanoparticles for Activated Photoacoustic Imaging and Photothermal Therapy of Tumors. Analytical Chemistry, 2021, 93, 9277-9285.	6.5	34
18	Sequential SPECT and NIR-II imaging of tumor and sentinel lymph node metastasis for diagnosis and image-guided surgery. Biomaterials Science, 2021, 9, 3069-3075.	5.4	14

#	Article	IF	CITATIONS
19	Anchoring Group Mediated Radiolabeling for Achieving Robust Nanoimaging Probes. Small, 2021, 17, e2104977.	10.0	11
20	Rational Constructed Ultra-Small Iron Oxide Nanoprobes Manifesting High Performance for T1-Weighted Magnetic Resonance Imaging of Glioblastoma. Nanomaterials, 2021, 11, 2601.	4.1	7
21	Rapidly liver-clearable rare-earth core–shell nanoprobe for dual-modal breast cancer imaging in the second near-infrared window. Journal of Nanobiotechnology, 2021, 19, 369.	9.1	8
22	Radiolabeling nanomaterials for multimodality imaging: New insights into nuclear medicine and cancer diagnosis. Biomaterials, 2020, 228, 119553.	11.4	109
23	Viscoelastic characterization of injured brain tissue after controlled cortical impact (CCI) using a mouse model. Journal of Neuroscience Methods, 2020, 330, 108463.	2.5	18
24	Boosting H ₂ O ₂ â€Guided Chemodynamic Therapy of Cancer by Enhancing Reaction Kinetics through Versatile Biomimetic Fenton Nanocatalysts and the Second Nearâ€Infrared Light Irradiation. Advanced Functional Materials, 2020, 30, 1906128.	14.9	177
25	NIR nanoprobe-facilitated cross-referencing manifestation of local disease biology for dynamic therapeutic response assessment. Chemical Science, 2020, 11, 803-811.	7.4	26
26	Biodegradable Inorganic Nanoparticles for Cancer Theranostics: Insights into the Degradation Behavior. Bioconjugate Chemistry, 2020, 31, 315-331.	3.6	82
27	Manganese-Mediated Growth of ZnS Shell on KMnF ₃ :Yb,Er Cores toward Enhanced Up/Downconversion Luminescence. ACS Applied Materials & Interfaces, 2020, 12, 11934-11944.	8.0	18
28	Doping Lanthanide Nanocrystals With Non-lanthanide Ions to Simultaneously Enhance Up- and Down-Conversion Luminescence. Frontiers in Chemistry, 2020, 8, 832.	3.6	21
29	Longer and Stronger: Improving Persistent Luminescence in Size-Tuned Zinc Gallate Nanoparticles by Alcohol-Mediated Chromium Doping. ACS Nano, 2020, 14, 12113-12124.	14.6	50
30	An MRI contrast agent based on a zwitterionic metal-chelating polymer for hepatorenal angiography and tumor imaging. Journal of Materials Chemistry B, 2020, 8, 6956-6963.	5.8	24
31	Engineering NIR-IIb fluorescence of Er-based lanthanide nanoparticles for through-skull targeted imaging and imaging-guided surgery of orthotopic glioma. Nano Today, 2020, 34, 100905.	11.9	100
32	Recent advances in molecular imaging of atherosclerotic plaques and thrombosis. Nanoscale, 2020, 12, 8040-8064.	5.6	38
33	Red blood cell membrane-coated upconversion nanoparticles for pretargeted multimodality imaging of triple-negative breast cancer. Biomaterials Science, 2020, 8, 1802-1814.	5.4	71
34	Ultra-sensitive Nanoprobe Modified with Tumor Cell Membrane for UCL/MRI/PET Multimodality Precise Imaging of Triple-Negative Breast Cancer. Nano-Micro Letters, 2020, 12, 62.	27.0	50
35	Metformin-Induced Stromal Depletion to Enhance the Penetration of Gemcitabine-Loaded Magnetic Nanoparticles for Pancreatic Cancer Targeted Therapy. Journal of the American Chemical Society, 2020, 142, 4944-4954.	13.7	153
36	Electrosprayed Soft Capsules of Millimeter Size for Specifically Delivering Fish Oil/Nutrients to the Stomach and Intestines. ACS Applied Materials & Interfaces, 2020, 12, 6536-6545.	8.0	27

#	Article	IF	CITATIONS
37	Chemodynamic Therapy: Boosting H ₂ O ₂ â€Guided Chemodynamic Therapy of Cancer by Enhancing Reaction Kinetics through Versatile Biomimetic Fenton Nanocatalysts and the Second Nearâ€Infrared Light Irradiation (Adv. Funct. Mater. 3/2020). Advanced Functional Materials, 2020, 30, 2070019.	14.9	2
38	Nanoparticles weaponized with builtâ€in functions for imagingâ€guided cancer therapy. View, 2020, 1, e19.	5.3	35
39	Optical/MRI dual-modality imaging of M1 macrophage polarization in atherosclerotic plaque with MARCO-targeted upconversion luminescence probe. Biomaterials, 2019, 219, 119378.	11.4	40
40	Self-Illuminating Agents for Deep-Tissue Optical Imaging. Frontiers in Bioengineering and Biotechnology, 2019, 7, 326.	4.1	23
41	Quantitatively Visualizing Tumor-Related Protease Activity <i>in Vivo</i> Using a Ratiometric Photoacoustic Probe. Journal of the American Chemical Society, 2019, 141, 3265-3273.	13.7	123
42	Boosting the Radiosensitizing and Photothermal Performance of Cu2–xSe Nanocrystals for Synergetic Radiophotothermal Therapy of Orthotopic Breast Cancer. ACS Nano, 2019, 13, 1342-1353.	14.6	91
43	Coordinatively Unsaturated Fe ³⁺ Based Activatable Probes for Enhanced MRI and Therapy of Tumors. Angewandte Chemie - International Edition, 2019, 58, 11088-11096.	13.8	143
44	Upconversion luminescence mediated photodynamic therapy through hydrophilically engineered porphyrin. Chemical Engineering and Processing: Process Intensification, 2019, 142, 107551.	3.6	9
45	Coordinatively Unsaturated Fe 3+ Based Activatable Probes for Enhanced MRI and Therapy of Tumors. Angewandte Chemie, 2019, 131, 11205-11213.	2.0	18
46	Light-Enhanced O ₂ -Evolving Nanoparticles Boost Photodynamic Therapy To Elicit Antitumor Immunity. ACS Applied Materials & Interfaces, 2019, 11, 16367-16379.	8.0	90
47	Rational Design and Synthesis of a Metalloproteinase-Activatable Probe for Dual-Modality Imaging of Metastatic Lymph Nodes in Vivo. Journal of Organic Chemistry, 2019, 84, 6126-6133.	3.2	25
48	Multispectral optoacoustic imaging of dynamic redox correlation and pathophysiological progression utilizing upconversion nanoprobes. Nature Communications, 2019, 10, 1087.	12.8	126
49	Second near-infrared photodynamic therapy and chemotherapy of orthotopic malignant glioblastoma with ultra-small Cu _{2â°'x} Se nanoparticles. Nanoscale, 2019, 11, 7600-7608.	5.6	100
50	Biocompatible off-stoichiometric copper indium sulfide quantum dots with tunable near-infrared emission <i>via</i> aqueous based synthesis. Chemical Communications, 2019, 55, 15053-15056.	4.1	24
51	Emitting/Sensitizing Ions Spatially Separated Lanthanide Nanocrystals for Visualizing Tumors Simultaneously through Up―and Down onversion Nearâ€Infrared II Luminescence In Vivo. Small, 2019, 15, e1905344.	10.0	41
52	Light-triggered crosslinking of gold nanoparticles for remarkably improved radiation therapy and computed tomography imaging of tumors. Nanomedicine, 2019, 14, 2941-2955.	3.3	7
53	Regional biomechanical imaging of liver cancer cells. Journal of Cancer, 2019, 10, 4481-4487.	2.5	10
54	Biocompatible near-infrared quantum dots delivered to the skin by microneedle patches record vaccination. Science Translational Medicine, 2019, 11, .	12.4	95

#	Article	IF	CITATIONS
55	Biocompatible Semiconductor Quantum Dots as Cancer Imaging Agents. Advanced Materials, 2018, 30, e1706356.	21.0	227
56	Timely Visualization of the Collaterals Formed during Acute Ischemic Stroke with Fe ₃ O ₄ Nanoparticleâ€based MR Imaging Probe. Small, 2018, 14, e1800573.	10.0	24
57	Characterizing viscoelastic properties of breast cancer tissue in a mouse model using indentation. Journal of Biomechanics, 2018, 69, 81-89.	2.1	27
58	Enhancing Both Biodegradability and Efficacy of Semiconducting Polymer Nanoparticles for Photoacoustic Imaging and Photothermal Therapy. ACS Nano, 2018, 12, 1801-1810.	14.6	299
59	Oral administration of highly bright Cr ³⁺ doped ZnGa ₂ O ₄ nanocrystals for <i>in vivo</i> targeted imaging of orthotopic breast cancer. Journal of Materials Chemistry B, 2018, 6, 1508-1518.	5.8	49
60	Recent advancements in biocompatible inorganic nanoparticles towards biomedical applications. Biomaterials Science, 2018, 6, 726-745.	5.4	121
61	Narrowing the Photoluminescence of Aqueous CdTe Quantum Dots via Ostwald Ripening Suppression Realized by Programmed Dropwise Precursor Addition. Journal of Physical Chemistry C, 2018, 122, 11109-11118.	3.1	16
62	Molecular mechanisms for delicately tuning the morphology and properties of Fe ₃ O ₄ nanoparticle clusters. CrystEngComm, 2018, 20, 2421-2429.	2.6	11
63	Dual-Ratiometric Target-Triggered Fluorescent Probe for Simultaneous Quantitative Visualization of Tumor Microenvironment Protease Activity and pH <i>in Vivo</i> . Journal of the American Chemical Society, 2018, 140, 211-218.	13.7	207
64	Biodegradable Nanoagents with Short Biological Half‣ife for SPECT/PAI/MRI Multimodality Imaging and PTT Therapy of Tumors. Small, 2018, 14, 1702700.	10.0	51
65	Detection of lymph node metastasis with near-infrared upconversion luminescent nanoprobes. Nanoscale, 2018, 10, 21772-21781.	5.6	28
66	Evaluation of the Laser-Induced Thermotherapy Treatment Effect of Breast Cancer Based on Tissue Viscoelastic Properties. Journal of Engineering and Science in Medical Diagnostics and Therapy, 2018, 1,	0.5	0
67	Halide perovskite nanocrystals can also stand luminescent in water. Science Bulletin, 2018, 63, 1241-1242.	9.0	2
68	Ultra-small nanocluster mediated synthesis of Nd 3+ -doped core-shell nanocrystals with emission in the second near-infrared window for multimodal imaging of tumor vasculature. Biomaterials, 2018, 175, 30-43.	11.4	81
69	Soybean Lecithinâ€Mediated Nanoporous PLGA Microspheres with Highly Entrapped and Controlled Released BMPâ€2 as a Stem Cell Platform. Small, 2018, 14, e1800063.	10.0	71
70	Enhanced Synergism of Thermo-chemotherapy For Liver Cancer with Magnetothermally Responsive Nanocarriers. Theranostics, 2018, 8, 693-709.	10.0	63
71	"Smart―Nanoprobes for Visualization of Tumor Microenvironments. Advanced Healthcare Materials, 2018, 7, e1800391.	7.6	47
72	Monitoring the Opening and Recovery of the Blood–Brain Barrier with Noninvasive Molecular Imaging by Biodegradable Ultrasmall Cu _{2–<i>x</i>} Se Nanoparticles. Nano Letters, 2018, 18, 4985-4992.	9.1	105

#	Article	IF	CITATIONS
73	A Novel Histochemical Staining Approach for Rareâ€Earthâ€Based Nanoprobes. Advanced Therapeutics, 2018, 1, 1800005.	3.2	11
74	MRI Probes: Timely Visualization of the Collaterals Formed during Acute Ischemic Stroke with Fe ₃ O ₄ Nanoparticleâ€based MR Imaging Probe (Small 23/2018). Small, 2018, 14, 1870108.	10.0	6
75	Materials aspects of semiconductor nanocrystals for optoelectronic applications. Materials Horizons, 2017, 4, 155-205.	12.2	78
76	Longitudinal Study of the Effects of Environmental pH on the Mechanical Properties of <i>Aspergillus niger</i> . ACS Biomaterials Science and Engineering, 2017, 3, 2974-2979.	5.2	5
77	Molecular Imaging of Vulnerable Atherosclerotic Plaques <i>in Vivo</i> with Osteopontin-Specific Upconversion Nanoprobes. ACS Nano, 2017, 11, 1816-1825.	14.6	91
78	Few‣ayer Graphdiyne Nanosheets Applied for Multiplexed Realâ€Time DNA Detection. Advanced Materials, 2017, 29, 1606755.	21.0	198
79	Tumor Microenvironmentâ€Triggered Aggregation of Antiphagocytosis ^{99m} Tcâ€Labeled Fe ₃ O ₄ Nanoprobes for Enhanced Tumor Imaging In Vivo. Advanced Materials, 2017, 29, 1701095.	21.0	162
80	An adaptive Fuzzy C-means method utilizing neighboring information for breast tumor segmentation in ultrasound images. Medical Physics, 2017, 44, 3752-3760.	3.0	35
81	Ultrasmall Magnetic CuFeSe ₂ Ternary Nanocrystals for Multimodal Imaging Guided Photothermal Therapy of Cancer. ACS Nano, 2017, 11, 5633-5645.	14.6	181
82	Diverse Applications of Nanomedicine. ACS Nano, 2017, 11, 2313-2381.	14.6	976
83	Lightâ€Triggered Assembly of Gold Nanoparticles for Photothermal Therapy and Photoacoustic Imaging of Tumors In Vivo. Advanced Materials, 2017, 29, 1604894.	21.0	444
84	Nanopolymersomes with an Ultrahigh Iodine Content for Highâ€Performance Xâ€Ray Computed Tomography Imaging In Vivo. Advanced Materials, 2017, 29, 1603997.	21.0	70
85	Monodisperse Dual Plasmonic Au@Cu _{2–<i>x</i>} E (E= S, Se) Core@Shell Supraparticles: Aqueous Fabrication, Multimodal Imaging, and Tumor Therapy at <i>in Vivo</i> Level. ACS Nano, 2017, 11, 8273-8281.	14.6	139
86	The Yin and Yang of coordinating co-solvents in the size-tuning of Fe ₃ O ₄ nanocrystals through flow synthesis. Nanoscale, 2017, 9, 18609-18612.	5.6	14
87	MRI/optical dual-modality imaging of vulnerable atherosclerotic plaque with an osteopontin-targeted probe based on Fe 3 O 4 nanoparticles. Biomaterials, 2017, 112, 336-345.	11.4	71
88	pHâ€Responsive Fe(III)–Gallic Acid Nanoparticles for In Vivo Photoacousticâ€Imagingâ€Guided Photothermal Therapy. Advanced Healthcare Materials, 2016, 5, 772-780.	7.6	94
89	Ultrasmall Biocompatible WO _{3â^'} <i>_x</i> Nanodots for Multiâ€Modality Imaging and Combined Therapy of Cancers. Advanced Materials, 2016, 28, 5072-5079.	21.0	227
90	Aqueous Based Semiconductor Nanocrystals. Chemical Reviews, 2016, 116, 10623-10730.	47.7	364

#	Article	IF	CITATIONS
91	Ambient Aqueous Synthesis of Ultrasmall PEGylated Cu _{2â^} <i>_x</i> Se Nanoparticles as a Multifunctional Theranostic Agent for Multimodal Imaging Guided Photothermal Therapy of Cancer. Advanced Materials, 2016, 28, 8927-8936.	21.0	282
92	Ultrasmall Biocompatible Bi ₂ Se ₃ Nanodots for Multimodal Imaging-Guided Synergistic Radiophotothermal Therapy against Cancer. ACS Nano, 2016, 10, 11145-11155.	14.6	196
93	Photothermal Therapy: Ambient Aqueous Synthesis of Ultrasmall PECylated Cu _{2â^'} <i>_x</i> Se Nanoparticles as a Multifunctional Theranostic Agent for Multimodal Imaging Guided Photothermal Therapy of Cancer (Adv. Mater. 40/2016). Advanced Materials. 2016. 28. 8788-8788.	21.0	6
94	Small is Smarter: Nano MRI Contrast Agents – Advantages and Recent Achievements. Small, 2016, 12, 556-576.	10.0	147
95	BSAâ€Mediated Synthesis of Bismuth Sulfide Nanotheranostic Agents for Tumor Multimodal Imaging and Thermoradiotherapy. Advanced Functional Materials, 2016, 26, 5335-5344.	14.9	255
96	In vivo covalent cross-linking of photon-converted rare-earth nanostructures for tumour localization and theranostics. Nature Communications, 2016, 7, 10432.	12.8	376
97	Differently sized magnetic/upconversion luminescent NaGdF ₄ :Yb,Er nanocrystals: flow synthesis and solvent effects. Chemical Communications, 2016, 52, 5872-5875.	4.1	28
98	Generation, Characterization, and Application of Hierarchically Structured Self-Assembly Induced by the Combined Effect of Self-Emulsification and Phase Separation. Journal of the American Chemical Society, 2016, 138, 2090-2093.	13.7	29
99	Detection of early primary colorectal cancer with upconversion luminescent NP-based molecular probes. Nanoscale, 2016, 8, 12579-12587.	5.6	36
100	Protease-Activated Ratiometric Fluorescent Probe for pH Mapping of Malignant Tumors. ACS Nano, 2015, 9, 3199-3205.	14.6	102
101	Flow Synthesis of Biocompatible Fe ₃ O ₄ Nanoparticles: Insight into the Effects of Residence Time, Fluid Velocity, and Tube Reactor Dimension on Particle Size Distribution. Chemistry of Materials, 2015, 27, 1299-1305.	6.7	64
102	Ultrasensitive <i>in Vivo</i> Detection of Primary Gastric Tumor and Lymphatic Metastasis Using Upconversion Nanoparticles. ACS Nano, 2015, 9, 2120-2129.	14.6	90
103	Insight into Strain Effects on Band Alignment Shifts, Carrier Localization and Recombination Kinetics in CdTe/CdS Core/Shell Quantum Dots. Journal of the American Chemical Society, 2015, 137, 2073-2084.	13.7	81
104	No king without a crown – impact of the nanomaterial-protein corona on nanobiomedicine. Nanomedicine, 2015, 10, 503-519.	3.3	101
105	Aqueous synthesis of PEGylated copper sulfide nanoparticles for photoacoustic imaging of tumors. Nanoscale, 2015, 7, 11075-11081.	5.6	68
106	Super-stable centimetre-scale inverse opal belts integrated with CdTe QDs for narrow band fluorescence optical waveguiding. Journal of Materials Chemistry C, 2015, 3, 10964-10967.	5.5	0
107	Chemical Spacer Design for Engineering the Relaxometric Properties of Core–Shell Structured Rare Earth Nanoparticles. Chemistry of Materials, 2015, 27, 7918-7925.	6.7	24
108	Imaging Tumor Metastases with Molecular Probes. Current Pharmaceutical Design, 2015, 21, 6260-6264.	1.9	6

#	Article	IF	CITATIONS
109	Are Rareâ€Earth Nanoparticles Suitable for In Vivo Applications?. Advanced Materials, 2014, 26, 6922-6932.	21.0	166
110	Nanocrystals: Restructuring and Remodeling of NaREF ₄ Nanocrystals by Electron Irradiation (Small 22/2014). Small, 2014, 10, 4800-4800.	10.0	0
111	Restructuring and Remodeling of NaREF ₄ Nanocrystals by Electron Irradiation. Small, 2014, 10, 4711-4717.	10.0	26
112	Upconversion luminescence nanoparticles-based lateral flow immunochromatographic assay for cephalexin detection. Journal of Materials Chemistry C, 2014, 2, 9637-9642.	5.5	48
113	Magnetically engineered Cd-free quantum dots as dual-modality probes for fluorescence/magnetic resonance imaging of tumors. Biomaterials, 2014, 35, 1608-1617.	11.4	110
114	Anchoring Group Effects of Surface Ligands on Magnetic Properties of Fe ₃ O ₄ Nanoparticles: Towards High Performance MRI Contrast Agents. Advanced Materials, 2014, 26, 2694-2698.	21.0	194
115	In situ111In-doping for achieving biocompatible and non-leachable 111In-labeled Fe3O4 nanoparticles. Chemical Communications, 2014, 50, 2170.	4.1	50
116	In vivo multimodality imaging of miRNA-16 iron nanoparticle reversing drug resistance to chemotherapy in a mouse gastric cancer model. Nanoscale, 2014, 6, 14343-14353.	5.6	54
117	Revisiting the coordination chemistry for preparing manganese oxide nanocrystals in the presence of oleylamine and oleic acid. Nanoscale, 2014, 6, 5918.	5.6	34
118	Detection of Epstein–Barr virus infection in cancer by using highly specific nanoprobe based on dBSA capped CdTe quantum dots. RSC Advances, 2014, 4, 22545.	3.6	9
119	Magnetically Engineered Semiconductor Quantum Dots as Multimodal Imaging Probes. Advanced Materials, 2014, 26, 6367-6386.	21.0	145
120	Nanoparticles: Are Rare-Earth Nanoparticles Suitable for In Vivo Applications? (Adv. Mater. 40/2014). Advanced Materials, 2014, 26, 6921-6921.	21.0	1
121	Facile synthesis of two-dimensional highly branched gold nanostructures in aqueous solutions of cationic gemini surfactant. CrystEngComm, 2013, 15, 2648.	2.6	21
122	Magnetic/Upconversion Fluorescent NaGdF ₄ :Yb,Er Nanoparticle-Based Dual-Modal Molecular Probes for Imaging Tiny Tumors <i>in Vivo</i> . ACS Nano, 2013, 7, 7227-7240.	14.6	336
123	Aqueous Manganese-Doped Core/Shell CdTe/ZnS Quantum Dots with Strong Fluorescence and High Relaxivity. Journal of Physical Chemistry C, 2013, 117, 18752-18761.	3.1	58
124	Bifunctional Superparticles Achieved by Assembling Fluorescent CuInS2@ZnS Quantum Dots and Amphibious Fe3O4Nanocrystals. Journal of Physical Chemistry C, 2013, 117, 21014-21020.	3.1	21
125	Ultra-Low-Field MRI and Spin-Lattice Relaxation Time of \$^{1}hbox{H}\$ in the Presence of \$hbox{Fe}_{3}hbox{O}_{4}\$ Magnetic Nano-Particles Detected With a High-\$T_{m C}\$ DC-SQUID. IEEE Transactions on Applied Superconductivity, 2013, 23, 1602504-1602504.	1.7	1
126	Template synthesis of braided gold nanowires with gemini surfactant–HAuCl4 aggregates. Journal of Nanoparticle Research, 2013, 15, 1.	1.9	13

#	Article	IF	CITATIONS
127	Cationic Gemini Surfactant-Assisted Synthesis of Hollow Au Nanostructures by Stepwise Reductions. ACS Applied Materials & Interfaces, 2013, 5, 5709-5716.	8.0	44
128	NaGdF ₄ Nanoparticle-Based Molecular Probes for Magnetic Resonance Imaging of Intraperitoneal Tumor Xenografts <i>in Vivo</i> . ACS Nano, 2013, 7, 330-338.	14.6	207
129	Ultrasmall PEGylated MnxFe3â^'xO4 (x = 0–0.34) nanoparticles: effects of Mn(ii) doping on T1- and T2-weighted magnetic resonance imaging. RSC Advances, 2013, 3, 23454.	3.6	19
130	Receptor-Mediated Delivery of Magnetic Nanoparticles across the Blood–Brain Barrier. ACS Nano, 2012, 6, 3304-3310.	14.6	272
131	Surface engineering of gold nanoparticles for in vitro siRNA delivery. Nanoscale, 2012, 4, 5102.	5.6	75
132	Synthesis of Cu ₃ SnS ₄ nanocrystals and nanosheets by using Cu ₃₁ S ₁₆ as seeds. CrystEngComm, 2012, 14, 401-404.	2.6	36
133	From Ultrathin Two-Dimensional Djurleite Nanosheets to One-Dimensional Nanorods Comprised of Djurleite Nanoplates: Synthesis, Characterization, and Formation Mechanism. Crystal Growth and Design, 2011, 11, 1109-1116.	3.0	22
134	Surface-biofunctionalized multicore/shell CdTe@SiO ₂ composite particles for immunofluorescence assay. Nanotechnology, 2011, 22, 505104.	2.6	18
135	Gelification: An Effective Measure for Achieving Differently Sized Biocompatible Fe ₃ O ₄ Nanocrystals through a Single Preparation Recipe. Journal of the American Chemical Society, 2011, 133, 19512-19523.	13.7	66
136	Aqueous synthesis of CdTe nanocrystals: progresses and perspectives. Chemical Communications, 2011, 47, 9293.	4.1	99
137	Facile synthesis of ultrasmall PEGylated iron oxide nanoparticles for dual-contrast <i>T</i> ₁ - and <i>T</i> ₂ -weighted magnetic resonance imaging. Nanotechnology, 2011, 22, 245604.	2.6	126
138	Lateral Flow Immunochromatographic Assay for Sensitive Pesticide Detection by Using Fe ₃ O ₄ Nanoparticle Aggregates as Color Reagents. Analytical Chemistry, 2011, 83, 6778-6784.	6.5	216
139	Quantum dot-antisense oligonucleotide conjugates for multifunctional gene transfection, mRNA regulation, and tracking of biological processes. Biomaterials, 2011, 32, 1923-1931.	11.4	40
140	Magnetic Iron Oxide Nanoparticles and Their Applications in Magnetic Resonance Imaging. Sheng Wu Wu Li Hsueh Bao, 2011, 27, 272-288.	0.1	7
141	One-pot synthesis of PVP-coated Ni0.6Fe2.4O4 nanocrystals. Science Bulletin, 2010, 55, 3472-3478.	1.7	5
142	Monodispersed Magnetic Polystyrene Beads with Excellent Colloidal Stability and Strong Magnetic Response. Macromolecular Rapid Communications, 2010, 31, 1805-1810.	3.9	16
143	Decorating multi-walled carbon nanotubes with quantum dots for construction of multi-color fluorescent nanoprobes. Nanotechnology, 2010, 21, 045606.	2.6	28
144	Synthesis, optical properties, and superlattice structure of Cu(I)-doped CdS nanocrystals. Applied Physics Letters, 2010, 97, .	3.3	56

#	Article	IF	CITATIONS
145	Penetration of Quantum Dot Particles Through Human Skin. Journal of Biomedical Nanotechnology, 2010, 6, 586-595.	1.1	60
146	Investigations on the Interactions between Plasma Proteins and Magnetic Iron Oxide Nanoparticles with Different Surface Modifications. Journal of Physical Chemistry C, 2010, 114, 21270-21276.	3.1	64
147	Highly Fluorescent CdTe@SiO ₂ Particles Prepared via Reverse Microemulsion Method. Chemistry of Materials, 2010, 22, 420-427.	6.7	107
148	Synthesis and self-assembly of Cu1.94S–ZnS heterostructured nanorods. CrystEngComm, 2010, 12, 4124.	2.6	54
149	Magnetic Janus Particles Prepared by a Flame Synthetic Approach: Synthesis, Characterizations and Properties. Advanced Materials, 2009, 21, 184-187.	21.0	103
150	Superparamagnetic iron oxide nanoparticles: from preparations to in vivo MRI applications. Journal of Materials Chemistry, 2009, 19, 6274.	6.7	610
151	A Novel Type of Dual-Modality Molecular Probe for MR and Nuclear Imaging of Tumor: Preparation, Characterization and in Vivo Application. Molecular Pharmaceutics, 2009, 6, 1074-1082.	4.6	79
152	Magnetic Ni/SiO2composite microcapsules prepared by one-pot synthesis. Journal of Materials Chemistry, 2009, 19, 1245-1251.	6.7	15
153	Polyhedral Maghemite Nanocrystals Prepared by a Flame Synthetic Method: Preparations, Characterizations, and Catalytic Properties. ACS Nano, 2009, 3, 1775-1780.	14.6	60
154	Investigation on Photovoltaic Performance based on Matchstick-Like Cu2S–In2S3 Heterostructure Nanocrystals and Polymer. Nanoscale Research Letters, 2008, 3, 502-507.	5.7	36
155	Superdispersible PVP-Coated Fe ₃ O ₄ Nanocrystals Prepared by a "One-Pot― Reaction. Journal of Physical Chemistry B, 2008, 112, 14390-14394.	2.6	115
156	Synthesis and Shape-Tailoring of Copper Sulfide/Indium Sulfide-Based Nanocrystals. Journal of the American Chemical Society, 2008, 130, 13152-13161.	13.7	246
157	Preparations of bifunctional polymeric beads simultaneously incorporated with fluorescent quantum dots and magnetic nanocrystals. Nanotechnology, 2008, 19, 105601.	2.6	48
158	Investigations on Iron Sulfide Nanosheets Prepared via a Single-Source Precursor Approach. Crystal Growth and Design, 2008, 8, 1023-1030.	3.0	119
159	A general approach for encapsulating aqueous colloidal particles into polymeric microbeads. Journal of Materials Chemistry, 2007, 17, 2930.	6.7	34
160	Coating Aqueous Quantum Dots with Silica via Reverse Microemulsion Method:  Toward Size-Controllable and Robust Fluorescent Nanoparticles. Chemistry of Materials, 2007, 19, 4123-4128.	6.7	176
161	Preparation of magnetite nanocrystals with surface reactive moieties by one-pot reaction. Journal of Colloid and Interface Science, 2007, 311, 469-474.	9.4	55
162	Detection of toxoplasmic lesions in mouse brain by USPIO-enhanced magnetic resonance imaging. Magnetic Resonance Imaging, 2007, 25, 1442-1448.	1.8	19

#	Article	IF	CITATIONS
163	A facile route for preparing rhabdophane rare earth phosphate nanorods. Journal of Materials Chemistry, 2006, 16, 1360.	6.7	69
164	Incorporating CdTe Nanocrystals into Polystyrene Microspheres: Towards Robust Fluorescent Beads. Small, 2006, 2, 898-901.	10.0	105
165	Shape controllable preparations of PbS nanocrystals using cysteine as the precursor of S2â^' ions. Science Bulletin, 2006, 51, 2576-2580.	1.7	3
166	Diameter-Tunable CdTe Nanotubes Templated by 1D Nanowires of Cadmium Thiolate Polymer. Angewandte Chemie - International Edition, 2006, 45, 6462-6466.	13.8	105
167	Preparation of bioconjugates of CdTe nanocrystals for cancer marker detection. Nanotechnology, 2006, 17, 2972-2977.	2.6	46
168	Preparation of Water-Soluble Magnetite Nanocrystals from Hydrated Ferric Salts in 2-Pyrrolidone: Mechanism Leading to Fe3O4. Angewandte Chemie - International Edition, 2005, 44, 123-126.	13.8	229
169	Amphiphilic ABC Triblock Copolymer-Assisted Synthesis of Core/Shell Structured CdTe Nanowires. Langmuir, 2005, 21, 4205-4210.	3.5	45
170	Size-Dependent Electrochemical Behavior of Thiol-Capped CdTe Nanocrystals in Aqueous Solution. Journal of Physical Chemistry B, 2005, 109, 1094-1100.	2.6	211
171	A Bio-inspired Route to Fabricate Submicrometer-Sized Particles with Unusual Shapes â^' Mineralization of Calcium Carbonate within Hydrogel Spheres. Chemistry of Materials, 2005, 17, 656-660.	6.7	57
172	Incorporating Fluorescent CdTe Nanocrystals into a Hydrogel via Hydrogen Bonding:Â Toward Fluorescent Microspheres with Temperature-Responsive Properties. Chemistry of Materials, 2005, 17, 2648-2653.	6.7	169
173	One-Pot Reaction to Synthesize Water-Soluble Magnetite Nanocrystals. Chemistry of Materials, 2004, 16, 1391-1393.	6.7	338
174	Enhancement Effect of Illumination on the Photoluminescence of Water-Soluble CdTe Nanocrystals: Toward Highly Fluorescent CdTe/CdS Core—Shell Structure ChemInform, 2004, 35, no.	0.0	0
175	Enhancement Effect of Illumination on the Photoluminescence of Water-Soluble CdTe Nanocrystals: Toward Highly Fluorescent CdTe/CdS Coreâ^'Shell Structure. Chemistry of Materials, 2004, 16, 3853-3859.	6.7	386
176	Preparation and photoluminescence of water-dispersible ZnSe nanocrystals. Materials Letters, 2004, 58, 3898-3902.	2.6	82
177	Synthesis and characterization of biodegradable poly(ester anhydride) based on É>-caprolactone and adipic anhydride initiated by potassium poly(ethylene glycol)ate. Journal of Polymer Science Part A, 2003, 41, 1511-1520.	2.3	5
178	The Influence of Carboxyl Groups on the Photoluminescence of Mercaptocarboxylic Acid-Stabilized CdTe Nanoparticles. Journal of Physical Chemistry B, 2003, 107, 8-13.	2.6	581
179	Site-Selective Deposition of Enzyme/Polyelectrolyte Multilayer Films on ITO Electrodes Controlled Electric Fields. Chemistry Letters, 2002, 31, 1168-1169.	1.3	9
180	Lateral Patterning of CdTe Nanocrystal Films by the Electric Field Directed Layer-by-Layer Assembly Method. Langmuir, 2002, 18, 4098-4102.	3.5	127

#	Article	IF	CITATIONS
181	Layer-by-layer depositions of polyelectrolyte/CdTe nanocrystal films controlled by electric fields. Journal of Materials Chemistry, 2002, 12, 1775-1778.	6.7	29
182	Electric Field Directed Layer-by-Layer Assembly of Highly Fluorescent CdTe Nanoparticles. Journal of Nanoscience and Nanotechnology, 2001, 1, 133-136.	0.9	70
183	Electroluminescence of different colors from polycation/CdTe nanocrystal self-assembled films. Journal of Applied Physics, 2000, 87, 2297-2302.	2.5	310
184	Layer-by-layer deposition of J-aggregates and polyelectrolytes for electroluminescence applications: A spectroscopic study. Israel Journal of Chemistry, 2000, 40, 129-138.	2.3	13
185	Synthesis and Characterization of a Size Series of Extremely Small Thiol-Stabilized CdSe Nanocrystals. Journal of Physical Chemistry B, 1999, 103, 3065-3069.	2.6	565
186	Electroluminescence and photoluminescence in CdSe/poly (p-phenylene vinylene) composite films. Synthetic Metals, 1999, 102, 1213-1214.	3.9	20
187	Strongly Photoluminescent CdTe Nanocrystals by Proper Surface Modification. Journal of Physical Chemistry B, 1998, 102, 8360-8363.	2.6	678
188	Electroluminescence Studies on Self-Assembled Films of PPV and CdSe Nanoparticles. Journal of Physical Chemistry B, 1998, 102, 4096-4103.	2.6	214
189	White-light electroluminescence from self-assembled Q-CdSe/PPV multilayer structures. Advanced Materials, 1997, 9, 802-805.	21.0	144
190	Assembly of modified CdS particles/cationic polymer based on electrostatic interactions. Thin Solid Films, 1996, 284-285, 242-245.	1.8	34
191	Effect of the surface chemical modification on the optical properties of polymer-stabilized PbS nanoparticles. Journal of the Chemical Society, Faraday Transactions, 1995, 91, 4121.	1.7	34
192	Polymer Langmuir-Blodgett film of organic-inorganic (Fe2O3) composite microgel. Thin Solid Films, 1994, 248, 106-109.	1.8	30
193	A monolayer of PbI2nanoparticles adsorbed on MD–LB film. Journal of the Chemical Society Chemical Communications, 1994, , 2229-2230.	2.0	40
194	Constructing PbI2 nanoparticles into a multilayer structure using the molecular deposition (MD) method. Journal of the Chemical Society Chemical Communications, 1994, , 2777.	2.0	59